

FIG 5 Amino acid alignment and hydrophobicity of EHcV and HCV core proteins. (A) Alignment of the core proteins of EHcV (JPN3/JAPAN/2013) and HCV genotype 1b (Con1; GenBank accession number [AJ238799](#)). Asterisks indicate identical amino acid residues. Bars indicate gaps to achieve maximum amino acid matching. The black and white arrowheads indicate the predicted cleavage site of the core protein of HCV by SPP and signal peptidase, respectively. The EHcV core protein was composed of three domains, domain 1 (a black line, residues 2 to 132), domain 2 (a broken black line, residues 133 to 187), and domain 3 (a gray line, residues 188 to 204), relative to those of the HCV core protein (42). (B) Hydrophobicity plots of the EHcV and HCV core proteins were prepared by the method of Kyte and Doolittle (26). The horizontal and vertical axes represent amino acid position and hydrophobicity, respectively.

HCV core protein and to be coprecipitated with the immature core protein (28). HCVc had a molecular mass of 23 kDa in the presence of wild-type SPP (SPP-wt) and was detected with the anti-FLAG antibody, but not with the anti-HA antibody (Fig. 6D, lane 2), suggesting that the 23-kDa protein band may be a mature core protein. HCVc mainly had a molecular mass of 28 kDa in the presence of SPP-D219A and was detected with the anti-FLAG and anti-HA antibodies (Fig. 6D, lane 3), which corresponds to the mobility of HCVc-mt (Fig. 6D, lane 4). These results suggest that SPP-D219A may abrogate the intramembrane cleavage of HCVc. In a manner similar to that for the HCV core protein, EHcVc was detected mainly at a molecular mass of 27 kDa in the presence of SPP-wt with the anti-FLAG antibody, but not with the anti-HA antibody (Fig. 6D, lane 6). EHcVc was detected mainly at a molecular mass of 30 kDa in the presence of SPP-D219A with anti-FLAG and anti-HA antibodies (Fig. 6D, lane 7), corresponding to the mobility of EHcVc-mt (Fig. 6D, lane 8). When SPP-D219A was coexpressed with either HCVc or EHcVc, immature HCVc and EHcVc were coprecipitated with SPP-D219A (Fig. 6E, lanes 3 and 5). These results suggest that the EHcV core protein may be cleaved by SPP and that Ile¹⁹⁰ and Phe¹⁹¹ of the EHcV core protein are critical for SPP-dependent cleavage.

The intracellular localization of the hepacivirus core protein.

The HCV core protein is known to be localized mainly on the surface of LDs and is partially fractionated in the detergent-resistant membrane (DRM) close to the budding sites on the ER (13, 14, 16, 17). The core protein is considered to encompass the viral genome on the ER membrane, followed by budding into the lu-

men side (13, 14, 16, 17). To examine the intracellular localization of the EHcV core protein, we expressed HCVc or EHcVc in the Huh7OK1 cell line and stained the core proteins with the anti-FLAG antibody after staining LDs. Consistent with the findings of previous studies (14, 41, 42), HCVc was localized mainly on LDs (Fig. 7, row 3), whereas HCVc-mt was not (Fig. 7, row 4). In a manner similar to that for the HCV core protein, EHcVc was localized mainly on LDs (Fig. 7, top row), whereas EHcVc-mt was not (Fig. 7, second row). These results suggest that the EHcV core protein may be localized mainly on LDs after SPP-dependent cleavage.

The DRM is defined as the cholesterol/sphingolipid-rich microdomain, which is resistant to nonionic detergents such as Triton X-100, considered to be a characteristic of lipid rafts. HCV was previously shown to be propagated in lipid raft-like compartments, including the membranous web (43–45). Furthermore, the HCV core protein is known to be associated with lipid raft-like compartments as well as LDs (16, 17, 41, 42). Therefore, we determined whether the EHcV core protein could be detected in the DRM fractions. EHcVc or EHcVc-mt was expressed in 293FT cells. The resulting cells were lysed on ice in the presence or absence of 1% Triton X-100. The DRM fractions were separated from the soluble proteins by a flotation assay with a stepwise density gradient in the presence or absence of Triton X-100. Serial fractions were collected after ultracentrifugation and were then subjected to Western blot analysis after being concentrated. EHcVc and EHcVc-mt were fractionated broadly from fractions of samples 3 to 11 without Triton X-100, and the fraction from

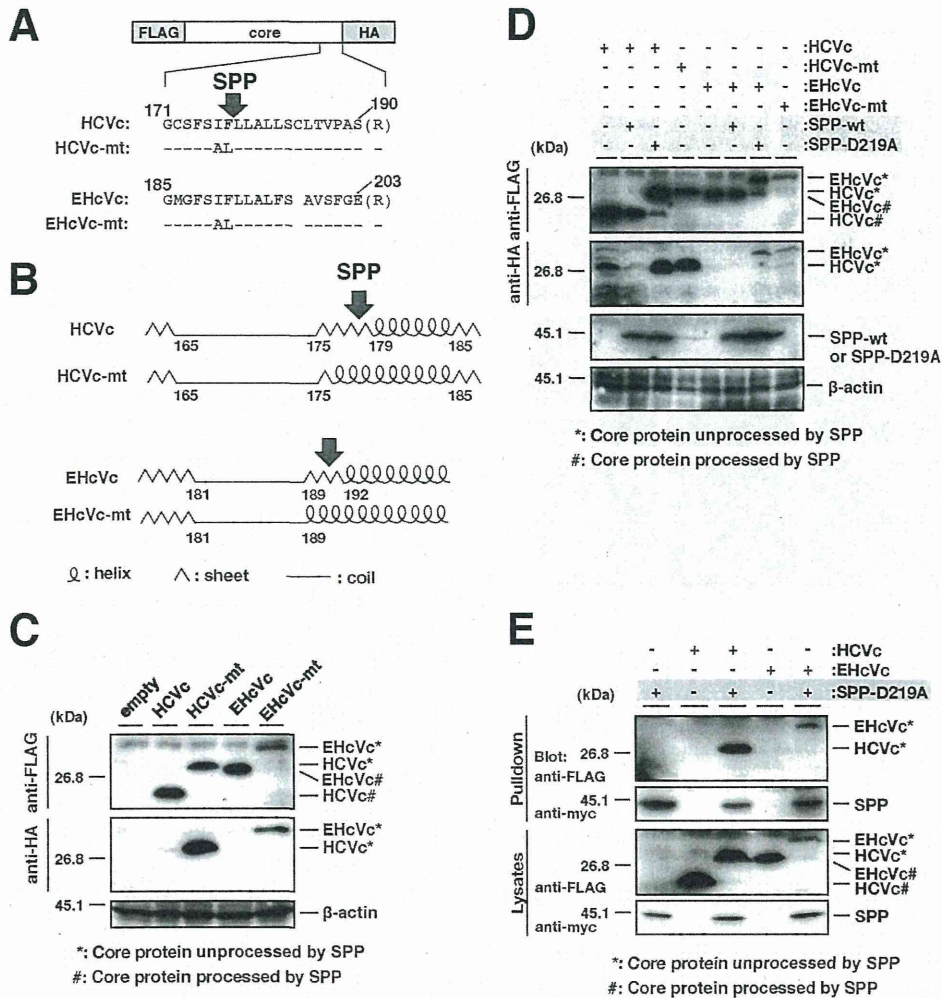


FIG 6 Intramembrane processing of the EHcV core protein by SPP. (A) The plasmids encoding HCVc, HCVc-mt, EHcVc, and EHcVc-mt are shown as a schematic diagram. Their C-terminal regions (171 to 190, HCVc core protein; 185 to 203, EHcVc core protein) were aligned. The C-terminal Ala of each core protein was replaced with Arg (R) to prevent signal peptidase-dependent cleavage for the detection of the SPP-uncleaved core protein with the anti-HA antibody. Bars indicate the amino acids that were the same as those of the wild-type residues. (B) The secondary protein structures in the C-terminal transmembrane regions of the HCVc and EHcVc core proteins and mutants were predicted by the method of Garnier et al. (25). Arrows indicate putative SPP cleavage sites. (C) HCVc, HCVc-mt, EHcVc, and EHcVc-mt were expressed in 293FT cells and immunoblotted with the anti-FLAG and -HA antibodies. (D) HCVc or EHcVc was expressed with SPP-wt or SPP-D219A in the 293FT cell line. HCVc-mt and EHcVc-mt were expressed in the absence of SPP-wt and SPP-D219A as uncleavable controls. (E) HCVc or EHcVc was coexpressed with or without SPP-D219A. SPP-D219A was pulled down with Ni beads. Coprecipitated proteins were immunoblotted with the anti-FLAG antibody.

sample 8 contained the largest amount of the core protein (Fig. 8, left panels). The distributions of the core proteins were roughly consistent with that of calreticulin, a marker protein of the ER membrane. When the cells expressing EHcVc were lysed in the presence of Triton X-100, a large amount of the core protein was localized in fractions 9 to 11 (Fig. 8, top three panels on the right). These fractions were enriched in calreticulin, corresponding to the detergent-soluble fractions (Fig. 8, fractions 7 to 11, top three panels on the right). However, EHcVc was partially detected in fractions 3 to 6 together with caveolin-1, a marker protein of the lipid raft (Fig. 8, fractions 3 to 6, top three panels on the right), suggesting that the EHcVc core protein may have been partially distributed in the DRM fractions. In contrast, EHcVc-mt was localized in the detergent-soluble fractions (Fig. 8, fractions 9 to 11, bottom three panels on the right), but not in the DRM fractions

(Fig. 8, fractions 3 to 6, bottom three panels on the right), in the presence of Triton X-100. EHcVc-mt was resistant to SPP-dependent processing, as described above (Fig. 6). These results suggest that the EHcVc core protein may have been partially localized in the DRM and also that SPP-dependent processing may be required for DRM localization of the EHcVc core protein.

DISCUSSION

The results of the present study indicate that EHcV infects Japanese-born domestic horses. Previous studies suggested that EHcV infected mainly horses and rarely dogs (5, 7–9). Our results demonstrate that EHcV commonly infects Japanese-born domestic horses (35.6% PCR positive and 22.6% seropositive). Several groups reported a prevalence of less than 10% PCR positivity in horses raised in the United States, the United Kingdom, and Ger-

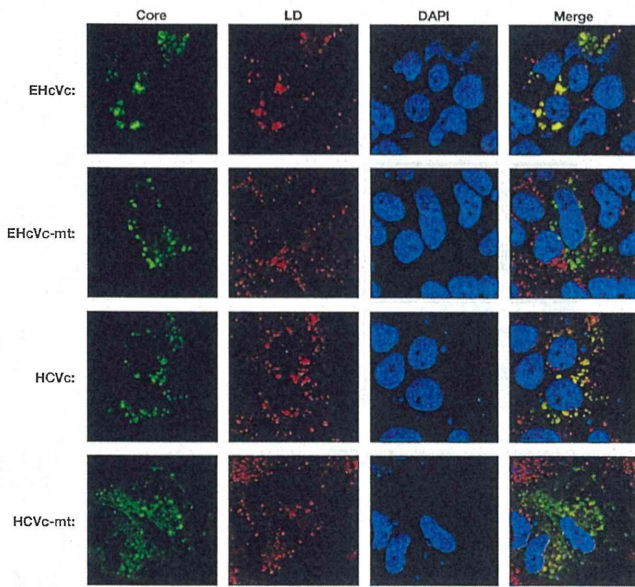


FIG 7 Intracellular localization of hepacivirus core proteins. HCVc, HCVc-mt, EHcVc, or EHcVc-mt was expressed in the Huh7OK1 cell line. The resulting cells were stained with Bodipy 558/568 (red) and then fixed with 4% paraformaldehyde at 24 h posttransfection, permeabilized, and subjected to indirect immunofluorescence staining. Each core protein was detected using mouse anti-FLAG antibodies and then Alexa 488-conjugated anti-mouse IgG (green). Cell nuclei were stained with DAPI after fixation (blue).

many (5, 7–9). Although the infection route of EHcV remains unknown, horses that were previously imported to Japan may be highly infected with EHcV. The serological prevalence in the present study appeared to be lower than that reported previously (8). A specific signal of the viral protein may be selected by Western blotting, used herein, rather than by the luciferase immunoprecipitation system, as reported previously (8), since the serum of each horse reacted to different proteins irrespective of the EHcV core protein (Fig. 2). The predicted full sequence of the EHcV strain amplified from serum sample 3 had high homology to those of the previously reported strains (Table 2). The polyproteins of previous strains had approximately 95% amino acid homology to one another irrespective of the area in which the horses originated,

suggesting that these strains may belong to the same virological species. The parents of horse number 3 were born in Japan, while its grandparents were imported from the United States and Canada. Unfortunately, the sera of the parents and grandparents were not obtained in the present study. The EHcV strains obtained from Japanese-born horses may have originated from the United States or Canada. Another possibility is that one species of EHcV may have recently been distributed worldwide.

The primary and secondary structures of both UTRs are conserved among HCV strains and are essential for replication and translation. Four major stem-loop (SL) motifs have been detected in the 5' UTR of the HCV genome, three SL structures of which are known to be required for IRES activity (46). Domain IIIId plays a crucial role in anchoring of the 40S ribosome for IRES activity (47). Domain IIIb and the four-way helical junction of domains IIIa, IIIb, and IIIc bind eukaryotic initiation factor 3 (eIF3) and form a ternary complex, thereby forming the 48S preinitiation complex on HCV RNA (48). Moreover, domain II is known to be required to enhance eIF5-mediated GTP hydrolysis and the release of eIF2 from the 48S complex (48). These equivalent motifs were observed in the predicted secondary structures of the 5' UTR of the reported EHcV strains (49), as well as in strain JPN3/JAPAN/2013 in the present study (Fig. 4C). A recent study demonstrated that the EHcV 5' UTR exhibited IRES-dependent translation activity (50); however, further studies are needed to fully understand the IRES activity of the EHcV 5' UTR.

SL motifs embedded in the NS5B-coding region and UTRs of the HCV genome are known to be associated with viral replication. Several studies found that the mutational disruption of the complement sequence between 5BSL3.2 and 3'SL2 inhibited HCV RNA replication (33, 51). Additionally, the apical loop of domain IIIId in the HCV 5' UTR was shown to interact with the bulge of 5BSL3.2, supporting IRES-dependent translation and viral RNA replication (34–36). The RNA secondary structures of the 3' UTR in the EHcV genome remained unknown due to limited information on its nucleotide sequence. 3' RACE using poly(U) polymerase was employed in the present study because the ordinary 3'-RACE reaction using poly(A) polymerase was stopped at the (A)-rich region of the EHcV 3' UTR. The nucleotide sequence of the EHcV 3' UTR was determined, and its RNA secondary structure was then predicted (Fig. 4B and C). The results of the present

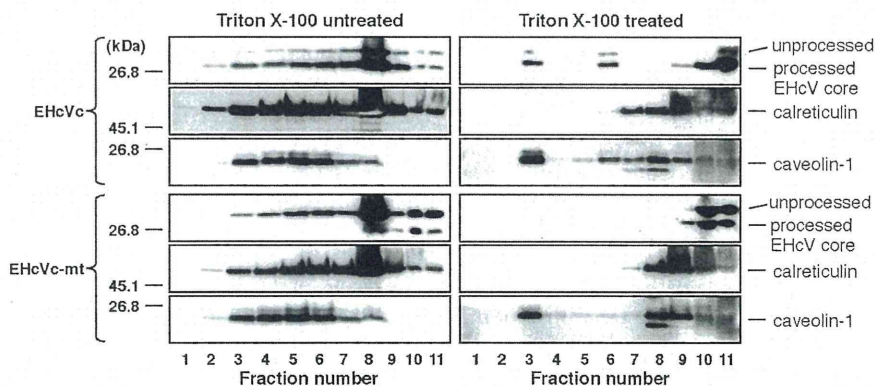


FIG 8 The EHcV core protein partially migrated to the DRM fraction after SPP-dependent processing. 293FT cells expressing either EHcVc or EHcVc-mt were homogenized with or without 1% Triton X-100 and then subjected to a flotation assay. Proteins in each fraction were concentrated with cold acetone and then subjected to Western blotting using the anti-FLAG, anti-calreticulin, or anti-caveolin-1 antibody.

study revealed that the 3' UTR of the EHcV genome consists of the (A)-rich sequence and relatively shorter 3'-X-tail sequence. The three SL structures of the EHcV 3' UTR were similar to those of the HCV 3' UTR but were markedly different from the 3' UTRs of GBV-B and rodent hepaciviruses. Drexler et al. described the structural characteristics of the 5' and 3' UTRs in rodent hepacivirus as well as phylogenetic information, liver tropism, and the pathogenicity of the virus (5). The SL motifs embedded in the 3' X-tails of rodent hepacivirus and GBV-B varied. The structures of the 3' UTRs appeared to correspond to the phylogenetic relationship of the hepaciviruses (5). Figure 4C shows that there were two stem-loop structures within the NS5B-coding region of EHcV corresponding to 5BSL3.2 and 5BSL3.3 of HCV RNA. Complementary regions were observed between the 5BSL3.2-like domain and 3'SL2, as well as between the 5BSL3.2-like domain and domain IIIId of the EHcV genome (Fig. 4B and C). The kissing-loop and long-range RNA-RNA interactions may be structurally conserved between EHcV and HCV. Functional analyses of the *cis*-acting elements of the EHcV genome will contribute to the establishment of an EHcV infection system.

The mature HCV core protein was previously shown to be generated from the viral precursor polyprotein by signal peptidase followed by SPP-dependent processing of the transmembrane region (52). The core proteins of HCV and GBV-B are known to be cleaved by SPP (12, 37). The transmembrane regions of both the HCV and EHcV core proteins were found to be structurally conserved, based on their amino acid sequences and hydrophobicity plots (Fig. 5A and B and Fig. 6B). The replacement of Ile¹⁹⁰ and Phe¹⁹¹ with Ala and Leu, respectively, in the EHcV core protein abrogated the intramembrane processing of the EHcV core protein (Fig. 6C). The loss-of-function mutant of SPP inhibited intramembrane processing of the EHcV core protein (Fig. 6D). Furthermore, the loss-of-function mutant of SPP specifically interacted with an uncleaved form of the EHcV core protein (Fig. 6E). These results indicate that the transmembrane region of the EHcV core protein may have been cleaved by SPP. The mature HCV core protein is known to be translocated into LDs and partially on lipid raft-like membranes. Previous studies reported that the HCV core protein on the LDs may be recruited near the replication complex in the membranous web, which consists of cholesterol- and sphingolipid-rich lipid components (43–45). Viral assembly was shown to occur on the ER membrane close to LDs and the membranous web (14). In addition to the HCV core protein, the nonstructural proteins and viral RNA of HCV were detected in the DRM fractions. The HCV RNA polymerase NS5B was previously reported to interact with sphingomyelin (53). Furthermore, a serine palmitoyltransferase inhibitor suppressed HCV replication by disrupting the replication complex (53, 54). These findings indicate that the DRM is provided as a scaffold for the formation of the HCV replication complex (45, 54). In the present study, we showed that the mature EHcV core protein was localized mainly on LDs and partially on the DRM (Fig. 7 and 8). A mutational analysis of the EHcV core protein indicated that SPP-dependent cleavage may be required for the localization of the EHcV core protein on LDs and the DRM in a manner similar to that for the HCV core protein. In addition, the assembly mechanism of EHcV may be similar to that of HCV.

In conclusion, the results of the present study show that EHcV shares common features with the HCV genomic structure and the biological properties of the capsid protein. *In vivo* and *ex vivo*

infection systems for EHcV have not yet been successfully established. SCID mice carrying chimeric human livers are currently employed as a small animal model for *in vivo* infection with HCV (55) but are not suitable for studies on immunity and pathogenicity due to an immunodeficiency. Chimpanzees are not yet available for *in vivo* HCV research. Further studies on the mechanisms underlying EHcV infection will contribute to the development of an *in vivo* surrogate model system for studying HCV immunity and pathogenicity.

ACKNOWLEDGMENTS

We thank M. Furugori for her secretarial work, I. Katoh for helpful discussions, and C. Endoh for technical assistance.

This work was supported by Grants-in-Aid from the Ministry of Health, Labor, and Welfare, Japan (H24-Kanen-008 and H25-Kanen-002 and -008); the Ministry of Education, Culture, Sports, Science, and Technology, Japan; and the Japan Science and Technology Agency (JST) (Houga-24659204).

REFERENCES

1. Simons JN, Leary TP, Dawson GJ, Pilot-Matias TJ, Muerhoff AS, Schlauder GG, Desai SM, Mushahwar IK. 1995. Isolation of novel virus-like sequences associated with human hepatitis. *Nat. Med.* 1:564–569. <http://dx.doi.org/10.1038/nm0695-564>.
2. Beames B, Chavez D, Lanford RE. 2001. GB virus B as a model for hepatitis C virus. *ILAR J.* 42:152–160. <http://dx.doi.org/10.1093/ilar.42.2.152>.
3. Bukh J, Apgar CL, Govindarajan S, Purcell RH. 2001. Host range studies of GB virus-B hepatitis agent, the closest relative of hepatitis C virus, in New World monkeys and chimpanzees. *J. Med. Virol.* 65:694–697. <http://dx.doi.org/10.1002/jmv.2092>.
4. Quan PL, Firth C, Conte JM, Williams SH, Zambrana-Torrel CM, Anthony SJ, Ellison JA, Gilbert AT, Kuzmin IV, Niezgodka M, Osinubi MO, Recuenco S, Markotter W, Breiman RF, Kalembe L, Malekani J, Lindblade KA, Rostal MK, Ojeda-Flores R, Suzan G, Davis LB, Blau DM, Ogunkoya AB, Alvarez Castillo DA, Moran D, Ngam S, Akaibe D, Agwanda B, Briese T, Epstein JH, Daszak P, Rupprecht CE, Holmes EC, Lipkin WI. 2013. Bats are a major natural reservoir for hepaciviruses and pegiviruses. *Proc. Natl. Acad. Sci. U. S. A.* 110:8194–8199. <http://dx.doi.org/10.1073/pnas.1303037110>.
5. Drexler JF, Corman VM, Muller MA, Lukashev AN, Gmyl A, Coutard B, Adam A, Ritz D, Leijten LM, van Riel D, Kallies R, Klose SM, Gloza-Rausch F, Binger T, Annan A, Adu-Sarkodie Y, Oppong S, Bourgarel M, Rupp D, Hoffmann B, Schlegel M, Kummerer BM, Kruger DH, Schmidt-Chanasit J, Setien AA, Cottontail VM, Hema-chudha T, Wacharapluesadee S, Osterrieder K, Bartenschlager R, Matthee S, Beer M, Kuiken T, Reusken C, Leroy EM, Ulrich RG, Drosten C. 2013. Evidence for novel hepaciviruses in rodents. *PLoS Pathog.* 9:e1003438. <http://dx.doi.org/10.1371/journal.ppat.1003438>.
6. Kapoor A, Simmonds P, Scheel TK, Hjelle B, Cullen JM, Burbelo PD, Chauhan LV, Duraisamy R, Sanchez Leon M, Jain K, Vandegriff KJ, Calisher CH, Rice CM, Lipkin WI. 2013. Identification of rodent homologs of hepatitis C virus and pegiviruses. *mBio* 4(2):e00216–13. <http://dx.doi.org/10.1128/mBio.00216-13>.
7. Lyons S, Kapoor A, Sharp C, Schneider BS, Wolfe ND, Culshaw G, Corcoran B, McGorum BC, Simmonds P. 2012. Nonprimate hepaciviruses in domestic horses, United Kingdom. *Emerg. Infect. Dis.* 18:1976–1982. <http://dx.doi.org/10.3201/eid1812.120498>.
8. Burbelo PD, Dubovi EJ, Simmonds P, Medina JL, Henriquez JA, Mishra N, Wagner J, Tokarz R, Cullen JM, Iadarola MJ, Rice CM, Lipkin WI, Kapoor A. 2012. Serology-enabled discovery of genetically diverse hepaciviruses in a new host. *J. Virol.* 86:6171–6178. <http://dx.doi.org/10.1128/JVI.00250-12>.
9. Kapoor A, Simmonds P, Gerold G, Qaisar N, Jain K, Henriquez JA, Firth C, Hirschberg DL, Rice CM, Shields S, Lipkin WI. 2011. Characterization of a canine homolog of hepatitis C virus. *Proc. Natl. Acad. Sci. U. S. A.* 108:11608–11613. <http://dx.doi.org/10.1073/pnas.1101794108>.
10. van der Laan LJ, de Ruiter PE, van Gils IM, Fieten H, Spee B, Pan Q, Rothuizen J, Penning LC. 5 June 2014. Canine hepacivirus and idiopathic

- hepatitis in dogs from a Dutch cohort. *J. Viral Hepat.* <http://dx.doi.org/10.1111/jvh.12268>.
11. Hüsey P, Langen H, Mous J, Jacobsen H. 1996. Hepatitis C virus core protein: carboxy-terminal boundaries of two processed species suggest cleavage by a signal peptide peptidase. *Virology* 224:93–104. <http://dx.doi.org/10.1006/viro.1996.0510>.
 12. Targett-Adams P, Schaller T, Hope G, Lanford RE, Lemon SM, Martin A, McLauchlan J. 2006. Signal peptide peptidase cleavage of GB virus B core protein is important for productive infection in vivo. *J. Biol. Chem.* 281:29221–29227. <http://dx.doi.org/10.1074/jbc.M605373200>.
 13. Hope RG, Murphy DJ, McLauchlan J. 2002. The domains required to direct core proteins of hepatitis C virus and GB virus-B to lipid droplets share common features with plant oleosin proteins. *J. Biol. Chem.* 277:4261–4270. <http://dx.doi.org/10.1074/jbc.M108798200>.
 14. Miyanari Y, Atsuzawa K, Usuda N, Watashi K, Hishiki T, Zayas M, Bartenschlager R, Wakita T, Hijikata M, Shimotohno K. 2007. The lipid droplet is an important organelle for hepatitis C virus production. *Nat. Cell Biol.* 9:1089–1097. <http://dx.doi.org/10.1038/ncb1631>.
 15. Samsa MM, Mondotte JA, Iglesias NG, Assuncao-Miranda I, Barbosa-Lima G, Da Poian AT, Bozza PT, Gamarnik AV. 2009. Dengue virus capsid protein usurps lipid droplets for viral particle formation. *PLoS Pathog.* 5:e1000632. <http://dx.doi.org/10.1371/journal.ppat.1000632>.
 16. Matto M, Rice CM, Aroeti B, Glenn JS. 2004. Hepatitis C virus core protein associates with detergent-resistant membranes distinct from classical plasma membrane rafts. *J. Virol.* 78:12047–12053. <http://dx.doi.org/10.1128/JVI.78.21.12047-12053.2004>.
 17. Okamoto K, Mori Y, Komoda Y, Okamoto T, Okochi M, Takeda M, Suzuki T, Moriishi K, Matsuura Y. 2008. Intramembrane processing by signal peptide peptidase regulates the membrane localization of hepatitis C virus core protein and viral propagation. *J. Virol.* 82:8349–8361. <http://dx.doi.org/10.1128/JVI.00306-08>.
 18. Aizaki H, Lee KJ, Sung VM, Ishiko H, Lai MM. 2004. Characterization of the hepatitis C virus RNA replication complex associated with lipid rafts. *Virology* 324:450–461. <http://dx.doi.org/10.1016/j.virol.2004.03.034>.
 19. Egger D, Wolk B, Gosert R, Bianchi L, Blum HE, Moradpour D, Bienz K. 2002. Expression of hepatitis C virus proteins induces distinct membrane alterations including a candidate viral replication complex. *J. Virol.* 76:5974–5984. <http://dx.doi.org/10.1128/JVI.76.12.5974-5984.2002>.
 20. Marchuk D, Drumm M, Saulino A, Collins FS. 1991. Construction of T-vectors, a rapid and general system for direct cloning of unmodified PCR products. *Nucleic Acids Res.* 19:1154. <http://dx.doi.org/10.1093/nar/19.5.1154>.
 21. Tajima S, Takasaki T, Matsuno S, Nakayama M, Kurane I. 2005. Genetic characterization of Yokose virus, a flavivirus isolated from the bat in Japan. *Virology* 332:38–44. <http://dx.doi.org/10.1016/j.virol.2004.06.052>.
 22. Tilgner M, Shi PY. 2004. Structure and function of the 3' terminal six nucleotides of the West Nile virus genome in viral replication. *J. Virol.* 78:8159–8171. <http://dx.doi.org/10.1128/JVI.78.15.8159-8171.2004>.
 23. Saitou N, Nei M. 1987. The neighbor-joining method: a new method for reconstructing phylogenetic trees. *Mol. Biol. Evol.* 4:406–425.
 24. Tamura K, Peterson D, Peterson N, Stecher G, Nei M, Kumar S. 2011. MEGA5: molecular evolutionary genetics analysis using maximum likelihood, evolutionary distance, and maximum parsimony methods. *Mol. Biol. Evol.* 28:2731–2739. <http://dx.doi.org/10.1093/molbev/msr121>.
 25. Garnier J, Osguthorpe DJ, Robson B. 1978. Analysis of the accuracy and implications of simple methods for predicting the secondary structure of globular proteins. *J. Mol. Biol.* 120:97–120. [http://dx.doi.org/10.1016/0022-2836\(78\)90297-8](http://dx.doi.org/10.1016/0022-2836(78)90297-8).
 26. Kyte J, Doolittle RF. 1982. A simple method for displaying the hydropathic character of a protein. *J. Mol. Biol.* 157:105–132. [http://dx.doi.org/10.1016/0022-2836\(82\)90515-0](http://dx.doi.org/10.1016/0022-2836(82)90515-0).
 27. Zuker M. 2003. Mfold web server for nucleic acid folding and hybridization prediction. *Nucleic Acids Res.* 31:3406–3415. <http://dx.doi.org/10.1093/nar/gkg595>.
 28. Okamoto K, Moriishi K, Miyamura T, Matsuura Y. 2004. Intramembrane proteolysis and endoplasmic reticulum retention of hepatitis C virus core protein. *J. Virol.* 78:6370–6380. <http://dx.doi.org/10.1128/JVI.78.12.6370-6380.2004>.
 29. Okamoto T, Nishimura Y, Ichimura T, Suzuki K, Miyamura T, Suzuki T, Moriishi K, Matsuura Y. 2006. Hepatitis C virus RNA replication is regulated by FKBP8 and Hsp90. *EMBO J.* 25:5015–5025. <http://dx.doi.org/10.1038/sj.emboj.7601367>.
 30. Honda M, Brown EA, Lemon SM. 1996. Stability of a stem-loop involving the initiator AUG controls the efficiency of internal initiation of translation on hepatitis C virus RNA. *RNA* 2:955–968.
 31. Yanagi M, St Claire M, Emerson SU, Purcell RH, Bukh J. 1999. In vivo analysis of the 3' untranslated region of the hepatitis C virus after in vitro mutagenesis of an infectious cDNA clone. *Proc. Natl. Acad. Sci. U. S. A.* 96:2291–2295. <http://dx.doi.org/10.1073/pnas.96.5.2291>.
 32. Blight KJ, Rice CM. 1997. Secondary structure determination of the conserved 98-base sequence at the 3' terminus of hepatitis C virus genome RNA. *J. Virol.* 71:7345–7352.
 33. Friebe P, Boudet J, Simorre JP, Bartenschlager R. 2005. Kissing-loop interaction in the 3' end of the hepatitis C virus genome essential for RNA replication. *J. Virol.* 79:380–392. <http://dx.doi.org/10.1128/JVI.79.1.380-392.2005>.
 34. Lourenço S, Costa F, Debarges B, Andrieu T, Cahour A. 2008. Hepatitis C virus internal ribosome entry site-mediated translation is stimulated by cis-acting RNA elements and trans-acting viral factors. *FEBS J.* 275:4179–4197. <http://dx.doi.org/10.1111/j.1742-4658.2008.06566.x>.
 35. Cristina J, del Pilar Moreno M, Moratorio G. 2007. Hepatitis C virus genetic variability in patients undergoing antiviral therapy. *Virus Res.* 127:185–194. <http://dx.doi.org/10.1016/j.virusres.2007.02.023>.
 36. Song Y, Friebe P, Tzima E, Junemann C, Bartenschlager R, Niepmann M. 2006. The hepatitis C virus RNA 3'-untranslated region strongly enhances translation directed by the internal ribosome entry site. *J. Virol.* 80:11579–11588. <http://dx.doi.org/10.1128/JVI.00675-06>.
 37. McLauchlan J, Lemberg MK, Hope G, Martoglio B. 2002. Intramembrane proteolysis promotes trafficking of hepatitis C virus core protein to lipid droplets. *EMBO J.* 21:3980–3988. <http://dx.doi.org/10.1093/emboj/cdf414>.
 38. Ogino T, Fukuda H, Imajoh-Ohmi S, Kohara M, Nomoto A. 2004. Membrane binding properties and terminal residues of the mature hepatitis C virus capsid protein in insect cells. *J. Virol.* 78:11766–11777. <http://dx.doi.org/10.1128/JVI.78.21.11766-11777.2004>.
 39. Kopp M, Murray CL, Jones CT, Rice CM. 2010. Genetic analysis of the carboxy-terminal region of the hepatitis C virus core protein. *J. Virol.* 84:1666–1673. <http://dx.doi.org/10.1128/JVI.02043-09>.
 40. Weihofen A, Binns K, Lemberg MK, Ashman K, Martoglio B. 2002. Identification of signal peptide peptidase, a presenilin-type aspartic protease. *Science* 296:2215–2218. <http://dx.doi.org/10.1126/science.1070925>.
 41. Barba G, Harper F, Harada T, Kohara M, Goulinet S, Matsuura Y, Eder G, Schaff Z, Chapman MJ, Miyamura T, Brechot C. 1997. Hepatitis C virus core protein shows a cytoplasmic localization and associates to cellular lipid storage droplets. *Proc. Natl. Acad. Sci. U. S. A.* 94:1200–1205. <http://dx.doi.org/10.1073/pnas.94.4.1200>.
 42. Hope RG, McLauchlan J. 2000. Sequence motifs required for lipid droplet association and protein stability are unique to the hepatitis C virus core protein. *J. Gen. Virol.* 81:1913–1925.
 43. Gao L, Aizaki H, He JW, Lai MM. 2004. Interactions between viral nonstructural proteins and host protein hVAP-33 mediate the formation of hepatitis C virus RNA replication complex on lipid raft. *J. Virol.* 78:3480–3488. <http://dx.doi.org/10.1128/JVI.78.7.3480-3488.2004>.
 44. Gosert R, Egger D, Lohmann V, Bartenschlager R, Blum HE, Bienz K, Moradpour D. 2003. Identification of the hepatitis C virus RNA replication complex in Huh-7 cells harboring subgenomic replicons. *J. Virol.* 77:5487–5492. <http://dx.doi.org/10.1128/JVI.77.9.5487-5492.2003>.
 45. Shi ST, Lee KJ, Aizaki H, Hwang SB, Lai MM. 2003. Hepatitis C virus RNA replication occurs on a detergent-resistant membrane that cofractionates with caveolin-2. *J. Virol.* 77:4160–4168. <http://dx.doi.org/10.1128/JVI.77.7.4160-4168.2003>.
 46. Tsukiyama-Kohara K, Iizuka N, Kohara M, Nomoto A. 1992. Internal ribosome entry site within hepatitis C virus RNA. *J. Virol.* 66:1476–1483.
 47. Babaylova E, Graifer D, Malygin A, Stahl J, Shatsky I, Karpova G. 2009. Positioning of subdomain IIIId and apical loop of domain II of the hepatitis C IRES on the human 40S ribosome. *Nucleic Acids Res.* 37:1141–1151. <http://dx.doi.org/10.1093/nar/gkn1026>.
 48. Kieft JS, Zhou K, Grech A, Jubin R, Doudna JA. 2002. Crystal structure of an RNA tertiary domain essential to HCV IRES-mediated translation initiation. *Nat. Struct. Biol.* 9:370–374. <http://dx.doi.org/10.1038/nsb781>.
 49. Locker N, Easton LE, Lukavsky PJ. 2007. HCV and CSFV IRES domain II mediate eIF2 release during 80S ribosome assembly. *EMBO J.* 26:795–805. <http://dx.doi.org/10.1038/sj.emboj.7601549>.

50. Stewart H, Walter C, Jones D, Lyons S, Simmonds P, Harris M. 2013. The non-primate hepacivirus 5' untranslated region possesses internal ribosomal entry site activity. *J. Gen. Virol.* 94:2657–2663. <http://dx.doi.org/10.1099/vir.0.055764-0>.
51. Diviney S, Tuplin A, Struthers M, Armstrong V, Elliott RM, Simmonds P, Evans DJ. 2008. A hepatitis C virus *cis*-acting replication element forms a long-range RNA-RNA interaction with upstream RNA sequences in NS5B. *J. Virol.* 82:9008–9022. <http://dx.doi.org/10.1128/JVI.02326-07>.
52. Penin F, Dubuisson J, Rey FA, Moradpour D, Pawlotsky JM. 2004. Structural biology of hepatitis C virus. *Hepatology* 39:5–19. <http://dx.doi.org/10.1002/hep.20032>.
53. Hirata Y, Ikeda K, Sudoh M, Tokunaga Y, Suzuki A, Weng L, Ohta M, Tobita Y, Okano K, Ozeki K, Kawasaki K, Tsukuda T, Katsume A, Aoki Y, Umehara T, Sekiguchi S, Toyoda T, Shimotohno K, Soga T, Nishijima M, Taguchi R, Kohara M. 2012. Self-enhancement of hepatitis C virus replication by promotion of specific sphingolipid biosynthesis. *PLoS Pathog.* 8:e1002860. <http://dx.doi.org/10.1371/journal.ppat.1002860>.
54. Katsume A, Tokunaga Y, Hirata Y, Munakata T, Saito M, Hayashi H, Okamoto K, Ohmori Y, Kusanagi I, Fujiwara S, Tsukuda T, Aoki Y, Klumpp K, Tsukiyama-Kohara K, El-Gohary A, Sudoh M, Kohara M. 2013. A serine palmitoyltransferase inhibitor blocks hepatitis C virus replication in human hepatocytes. *Gastroenterology* 145:865–873. <http://dx.doi.org/10.1053/j.gastro.2013.06.012>.
55. Mercer DF, Schiller DE, Elliott JF, Douglas DN, Hao C, Rinfret A, Addison WR, Fischer KP, Churchill TA, Lakey JR, Tyrrell DL, Kneteman NM. 2001. Hepatitis C virus replication in mice with chimeric human livers. *Nat. Med.* 7:927–933. <http://dx.doi.org/10.1038/90968>.

Original Article

Liver stiffness measurement for risk assessment of hepatocellular carcinoma

Akihisa Tatsumi,¹ Shinya Maekawa,¹ Mitsuaki Sato,¹ Nobutoshi Komatsu,¹ Mika Miura,¹ Fumitake Amemiya,² Yasuhiro Nakayama,¹ Taisuke Inoue,¹ Minoru Sakamoto¹ and Nobuyuki Enomoto¹¹First Department of Medicine, University of Yamanashi, Chuo, and ²Department of Gastroenterological Medicine, Kofu Municipal Hospital, Kofu, Yamanashi, Japan

Aim: Liver fibrosis is a risk factor for hepatocellular carcinoma (HCC), but at what fibrotic stage the risk for HCC is increased has been poorly investigated quantitatively. This study aimed to determine the appropriate cut-off value of liver stiffness for HCC concurrence by FibroScan, and its clinical significance in hepatitis B virus (HBV), hepatitis C virus (HCV) and non-B, non-C (NBNC) liver disease.

Methods: Subjects comprised 1002 cases (246 with HCC and 756 without HCC) with chronic liver disease (HBV, 104; HCV, 722; and NBNC, 176).

Results: Liver stiffness was significantly greater in all groups with HCC, and the determined cut-off value for HCC concurrence was more than 12.0 kPa in those with HCV, more than 8.5 kPa in those with HBV and more than 12.0 kPa in those with NBNC. Liver stiffness of more than 12.0 kPa was an inde-

pendent risk factor for new HCC development in HCV. For HCV, risk factors for HCC concurrence were old age, male sex, low albumin, low platelets and liver stiffness, while for HBV they were old age, low platelets and liver stiffness, and for NBNC they were old age, elevated α -fetoprotein and liver stiffness.

Conclusion: Liver stiffness cut-off values and their association with HCC concurrence were different depending on the etiology. In HCV, liver stiffness of more than 12.0 kPa was an independent risk factor for new HCC development. Collectively, determining the fibrotic cut-off values for HCC concurrence would be important in evaluating HCC risks.

Key words: FibroScan, hepatocellular carcinoma, liver fibrosis

INTRODUCTION

HEPATOCELLULAR CARCINOMA (HCC) is the fifth most common cancer in the world and the third most common cause of cancer deaths.¹ HCC, accounting for 90% of primary liver cancer, is a global clinical issue.² For improvement in the prognosis of

HCC, curative therapy following early detection is important. To this end, it is critical to identify high-risk groups for HCC and perform appropriate surveillance in the clinical practice of chronic liver disease. It has been postulated that hepatitis virus infection, old age, male sex, alanine aminotransferase (ALT) elevation, liver fibrosis, and low albumin (Alb), low platelets (Plt) and α -fetoprotein (AFP) elevation are risk factors for HCC; however, liver fibrosis is the most important risk factor irrespective of its etiology.³⁻⁶

To date, liver fibrosis has been evaluated by liver biopsy, but it is associated with several problems such as invasiveness, sampling errors, semiquantitation and diagnostic differences among pathologists. With the development of FibroScan (Echosens, Paris, France) using transient elastography, it has become possible to quantitate liver elasticity non-invasively.⁷ The diagnostic accuracy of FibroScan for liver fibrosis has been recognized widely for various chronic liver diseases with the exception of some liver conditions such as congestion,

Correspondence: Dr Nobuyuki Enomoto, First Department of Medicine, University of Yamanashi, 1110 Shimokato, Chuo, Yamanashi 409-3898, Japan. Email: enomoto@yamanashi.ac.jp

Financial disclosure: This study was supported in part by Grants-in-Aid from the Ministry of Education, Science, Sports and Culture of Japan (23390195, 23791404, 24590964 and 24590965), and in part by Grants-in-Aid from the Ministry of Health, Labour and Welfare of Japan (H23-kanen-001, H23-kanen-004, H23-kanen-006, H24-kanen-002, H24-kanen-004 and H25-kanen-006).

Received 27 December 2013; revision 22 May 2014; accepted 14 June 2014.

severe inflammation or cholestasis in which liver fibrosis might be overestimated with FibroScan.⁸⁻¹² The risk for HCC is evaluable based on liver stiffness measured by FibroScan in cases with hepatitis B virus (HBV) and hepatitis C virus (HCV).¹²⁻¹⁹ Nevertheless, in most reports the risk for HCC was only indirectly evaluated based on the value for liver cirrhosis as measured by FibroScan. Liver stiffness related to HCC has not been directly evaluated. Furthermore, the utility of FibroScan in evaluation of the risk for HCC has not been elucidated in non-B, non-C (NBNC) liver disease.

In this study, liver stiffness in patients with chronic liver disease was quantitatively measured and liver stiffness related to HCC occurrence was elucidated separately in cases with HCV, HBV and NBNC liver disease for investigations of its clinical utility.

METHODS

Patients

THE SUBJECTS COMPRISED 1002 patients with chronic liver disease whose liver stiffness was measured by FibroScan consecutively at the University of Yamanashi Hospital between January 2010 and December 2012. Informed consent had been obtained for measurement of liver stiffness before the modality was approved by the national insurance in October 2011. The HCV group (722 cases including 66 sustained virological response [SVR] cases), HBV group (104 cases) and NBNC group (176 cases) were defined as HCV antibody positive, hepatitis B surface antigen (HBsAg) positive, and HBsAg negative and HCV antibody negative cases, respectively. Both HBsAg and HCV antibody positive cases ($n=3$) and HIV co-infection cases (co-infection with HBV, $n=1$) were excluded. HCC cases included those with a history of HCC. Among the 1002 cases with chronic liver disease, 246 had HCC and 756 were without HCC. Of those without HCC, 470 hepatitis C cases were followed up by abdominal ultrasonography, contrast computed tomography (CT) or ethoxybenzyl (EOB) contrast magnetic resonance imaging (MRI) every 3–6 months. HCC was diagnosed by contrast ultrasonography, contrast enhancement in the arterial phase and poor enhancement at the equilibrium phase in contrast CT (including CT arteriography and computed tomographic arterial portography) and contrast MRI, and histology by liver tumor biopsy. According to the Declaration of Helsinki, this study was performed after approval was obtained by the ethical committee of the Faculty of Medicine, University of Yamanashi.

Measurement of liver stiffness

FibroScan502 (Echosens) was used for measurement with the M-probe and L-probe. Patients were placed in a supine position with the right hand at the most abducted position for right intercostal scanning. When at least 10 effective measurements were obtained with effective measurement at 60% or higher and interquartile range at less than 30%, such measurements were defined as effective and the median was employed as the result of the measurement.²⁰

Analytical methods

In each group of liver diseases (HCV, HBV and NBNC), liver stiffness was compared between patients with and without HCC. Then, the cut-off value of liver stiffness for diagnosis of HCC was determined for later analysis in each group. Patients' backgrounds, laboratory data and liver stiffness in the HCV, HBV and NBNC groups were subjected to univariate, multivariate and subgroup analyses on the relationship with HCC. The 470 HCV patients without HCC at enrollment were followed up with the day of measurement of liver stiffness designated as day 0. Factors related to the development of HCC were examined by univariate and multivariate analyses using values for liver stiffness and blood test results at enrollment.

Statistical analysis

Category data were analyzed by the χ^2 -test and Fisher's exact test, while numerical data were examined by Mann-Whitney *U*-test. The cut-off value was set to yield the largest Youden index by receiver-operator curve (ROC) analysis. Multiple logistic analysis was performed for multivariate analysis on factors related to HCC concurrence. The Cox regression hazard model was employed for multivariate analysis of factors related to HCC development. Yearly development of HCC was expressed as per person-year. Cumulative incidence of HCC development was calculated by the Kaplan-Meier curve. *P*-values less than 0.05 were considered significant.

RESULTS

Baseline characteristics

CLINICAL BACKGROUND FACTORS of 1002 patients were compared between patients with and without HCC according to group (Table 1). There were 722 cases in the HCV group, 104 in the HBV group and 176 in the NBNC group. For all groups there was a significant association with older age, low Alb and Plt,

Table 1 Baseline characteristics of patients with and without HCC

Factors	HCV patients (n = 722)			HBV patients (n = 104)			NBNC patients (n = 176)		
	HCC(+) (n = 167)	HCC(-) (n = 555)	P	HCC(+) (n = 29)	HCC(-) (n = 75)	P	HCC(+) (n = 50)	HCC(-) (n = 126)	P
Age (years)	72 (42-89)	61 (20-89)	<0.01	62 (49-76)	52 (19-73)	<0.01	70 (53-88)	63 (19-88)	<0.01
Sex (male/female)	111/56	288/266	<0.01	23/6	47/28	0.11	33/17	69/58	0.16
Alb (g/dL)	3.6 (1.8-5.1)	4.3 (2.1-5.3)	<0.01	4.4 (2.0-5.0)	4.5 (3.5-5.2)	0.04	3.8 (1.9-4.7)	4.1 (2.4-5.5)	<0.01
T-Bil (mg/dL)	0.8 (0.3-4.7)	0.7 (0.2-26.9)	<0.01	0.7 (0.3-1.2)	0.7 (0.2-1.6)	0.45	0.7 (0.1-1.5)	0.7 (0.1-2.3)	0.90
AST (U/L)	48 (13-340)	32 (8-262)	<0.01	28 (16-95)	25 (14-178)	0.06	43 (17-146)	32 (10-291)	0.03
ALT (U/L)	43 (4-557)	32 (2-334)	<0.01	25 (10-134)	21 (9-375)	0.13	29 (10-80)	29 (6-517)	0.99
γ-GT (U/L)	36 (11-918)	28 (9-354)	<0.01	56 (13-267)	21 (8-222)	<0.01	74 (15-628)	55 (7-743)	0.14
Plt (10 ⁹ /L)	94 (25-299)	157 (40-343)	<0.01	118 (21-207)	172.5 (58-300)	<0.01	117 (14-264)	168 (30-387)	<0.01
AFP (ng/mL)	12.9 (1.3-54 923)	3.6 (0.8-839)	<0.01	3.8 (1.3-22 421)	2.7 (1.1-70.9)	<0.01	5.8 (1.3-5194)	3.2 (0.8-25.3)	<0.01
Stiffness (kPa)	21.3 (3.9-75.0)	7.8 (3.0-72.0)	<0.01	9.2 (4.7-75.0)	5.6 (2.8-32.4)	<0.01	15.6 (3.3-75.0)	7.4 (2.8-66.4)	<0.01
Hx of IFN Tx (yes/no)	38/129	153/402	0.21	-	-	-	-	-	-
SVR/non-SVR	10/34	56/97	0.09	-	-	-	-	-	-
Tx of NA	-	-	-	16/13	34/41	0.37	-	-	-
HBV-DNA >4 log copies/mL	-	-	-	4/25	16/59	0.38	-	-	-

Values are expressed as the mean (range).

-, Not applicable; AFP, α-fetoprotein; Alb, albumin; ALT, alanine aminotransferase; AST, aspartate aminotransferase; HBV patients, HBs antigen positive patients; HCC, hepatocellular carcinoma; HCV patients, HCV antibody positive patients; Hx, history; IFN, interferon; NA, nucleoside analog; NBNC patients, HBs antigen negative and HCV antibody negative patients; Plt, platelet count; stiffness, liver stiffness; SVR, sustained virological response; T-Bil, total bilirubin; Tx, Treatment; γ-GT, γ-glutamyl transpeptidase.

and elevated AFP among those with HCC. The proportion of males was significantly higher among the HCC cases in the HCV group. Stiffness of the liver was significantly greater among the HCC cases in all groups.

Determining cut-off values related to HCC concurrence in each disease group

The cut-off value most related to HCC concurrence was determined by the ROC analysis in each disease group. It was set at more than 12.0 kPa (>12.0 kPa vs ≤12.0 kPa; odds ratio [OR], 14.7; $P < 0.001$) in the HCV group, at more than 8.5 kPa (>8.5 kPa vs ≤8.5 kPa; OR, 8.28; $P < 0.001$) in the HBV group and at more than 12.0 kPa (>12.0 kPa vs ≤12.0 kPa; OR, 4.67; $P < 0.001$) in the NBNC group (Fig. 1).

HCC concurrence-related factors

Hepatocellular carcinoma concurrence-related factors in the HCV group were examined. Univariate analysis revealed that age, sex, Alb, total bilirubin, aspartate aminotransferase (AST), γ -glutamyltransferase (γ -GT), Plt, AFP and liver stiffness of more than 12.0 kPa were significant factors (Table 2). With the significant factors extracted by univariate analysis, multivariate analysis was performed, and age, sex, Alb, Plt and liver stiffness of more than 12.0 kPa were independent factors

(Table 3). Liver stiffness of more than 12.0 kPa was significant with an OR of 4.53 ($P < 0.001$).

Hepatitis C virus patients were categorized into two groups according to liver stiffness of 12.0 kPa or less, and more than 12.0 kPa, and HCC concurrence-related factors were examined in each group. Multivariate analysis extracted age, sex, Alb and AFP in the group with liver stiffness of 12.0 kPa or less as independent factors, and age, Alb and Plt in the group with liver stiffness of more than 12.0 kPa (Table 3).

In the HBV group, HCC concurrence-related factors were examined. Univariate analysis revealed that age, Alb, γ -GT, Plt, AFP and liver stiffness of more than 8.5 kPa were significant factors (Table 2), and multivariate analysis extracted age as an independent factor (OR, 1.12 [range, 1.04–1.21], $P < 0.004$) while low Plt tended to be associated with a high risk for HCC occurrence (OR, 0.99 [range, 0.98–1.00], $P = 0.08$) (data not shown). Subgroup analysis showed that liver stiffness of more than 8.5 kPa was a significant factor for HCC concurrence irrespective of age of more than 60 years or 60 years or less, and Plt less than $150 \times 10^9/L$ or $150 \times 10^9/L$ or more (Fig. 2).

Also examined were HCC concurrence-related factors in the NBNC group. Univariate analysis revealed that Alb, Plt, AFP and liver stiffness of more than 12.0 kPa

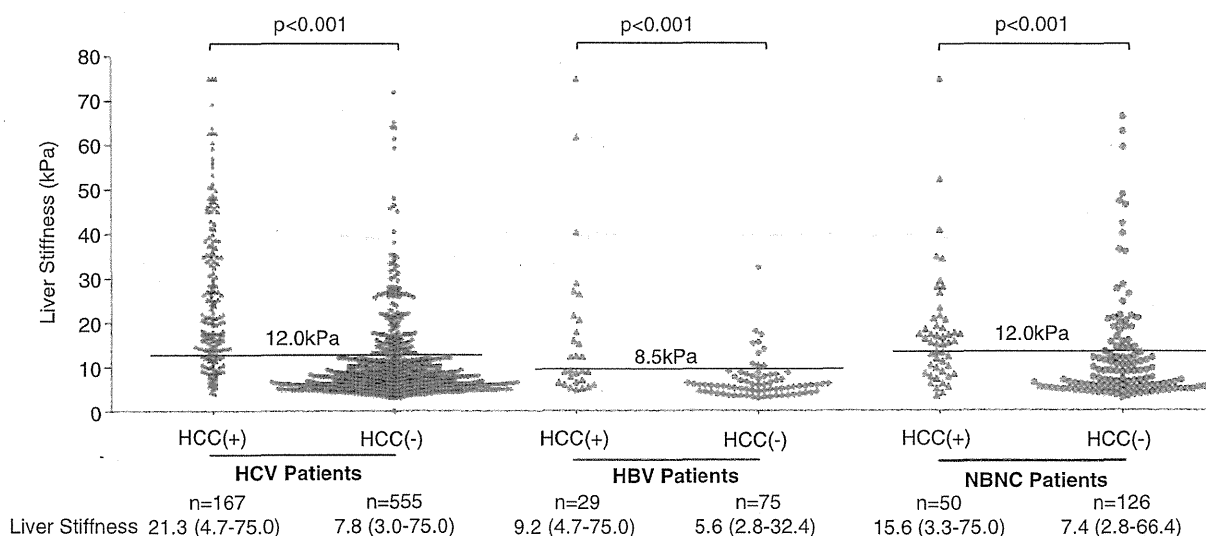


Figure 1 Distribution of liver stiffness categorized by the presence of hepatocellular carcinoma (HCC). Distribution of liver stiffness is shown in cases with liver disease of different etiologies with and without HCC. The cut-off value for liver stiffness was calculated so that sensitivity plus specificity would be the largest. A horizontal line indicating the cut-off value was drawn separately in each etiology group with an insertion of the value. Liver stiffness is shown as the median (range). Liver stiffness scores were significantly higher in cases with HCC concurrence. HBV, hepatitis B virus; HCV, hepatitis C virus; NBNC, non-B, non-C.